Supplementary information

Photo-transformation of Effluent Organic Matter by ZnO-based Sunlight Irradiation

Thao Thi Nguyen [1], Seong-Nam Nam [1,*] and Jeill Oh [1,*]

[1] Department of Civil and Environmental Engineering, Chung-Ang University, 84 Heukseok-ro, Dongjak-gu, Seoul, 06974, Republic of Korea; nguyenthithao4292@gmail.com; namsn76@gmail.com; ohjeill@cau.ac.kr

* Correspondence: namsn76@gmail.com (S.-N.N.); ohjeill@cau.ac.kr (J.O.);

List of Figures

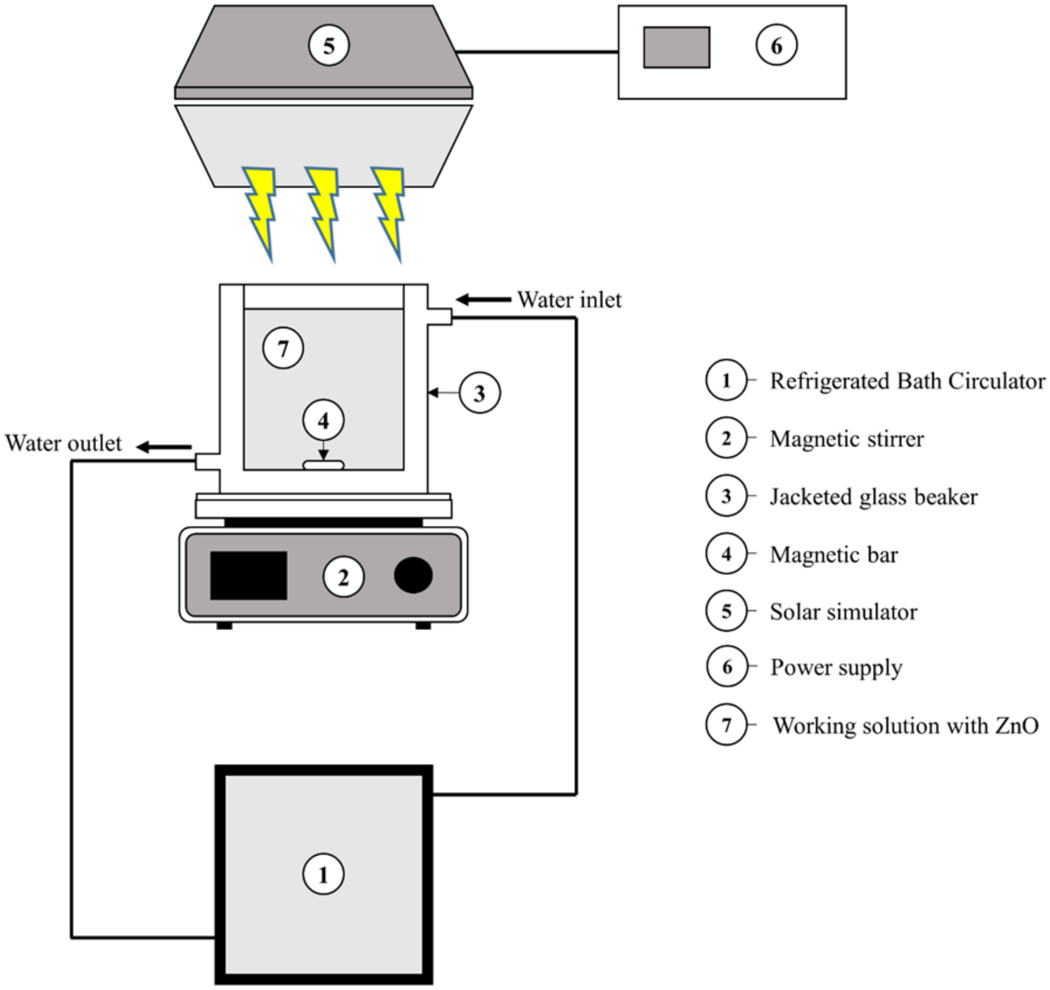

Figure S1. Experimental setup for the sunlight-induced photocatalytic degradation of organic matter present in receiving waters using ZnO as a photocatalyst.

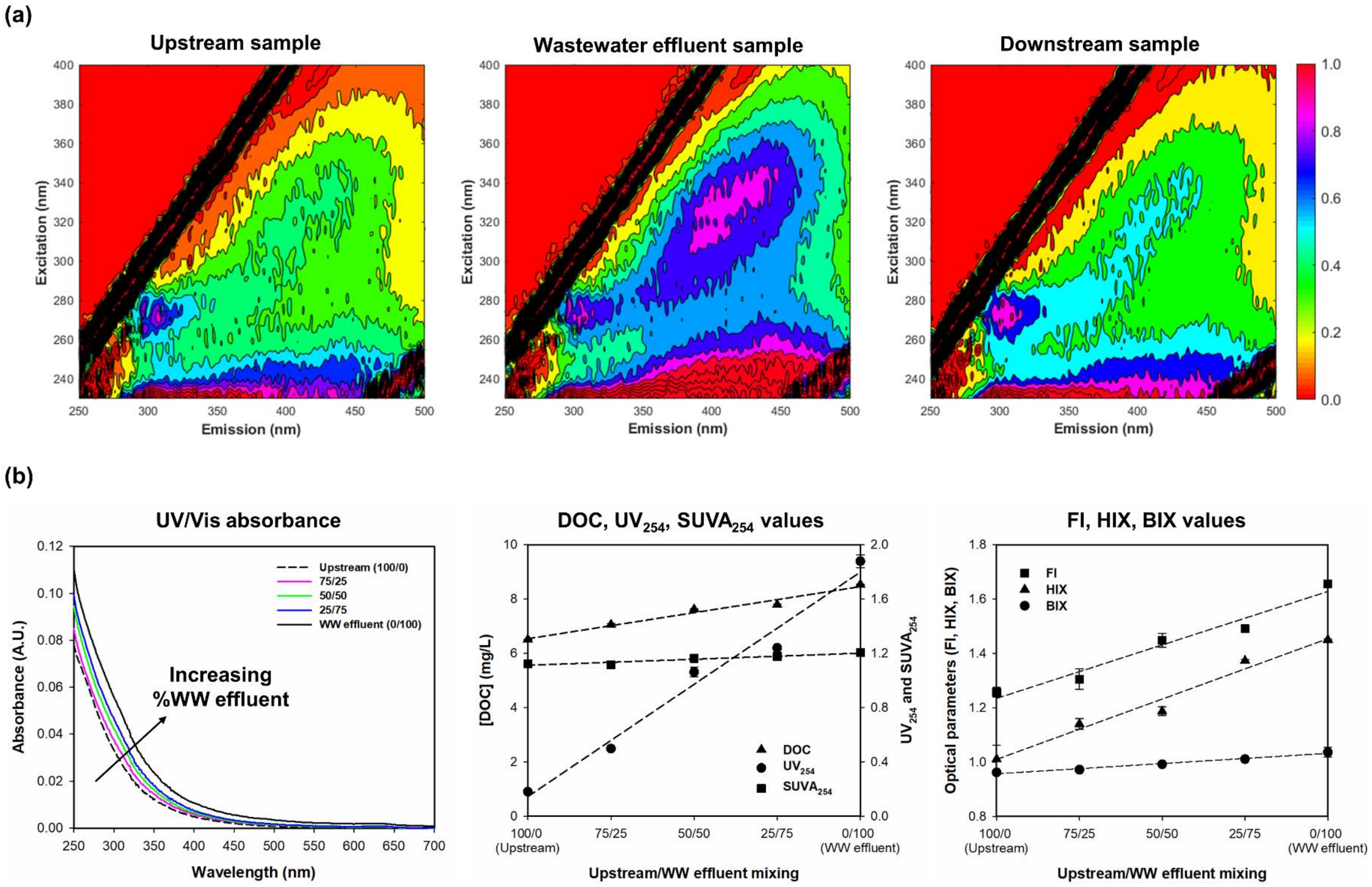

Figure S2. The UV/Vis absorption and EEM fluorescence spectrum for upstream, wastewater effluent, and downstream samples: (**a**) Fluorescence EEM spectra and (**b**) Changes in UV/Vis absorption spectra, DOC, UV_{254}, $SUVA_{254}$, FI, HIX, and BIX during the mixing between upstream and wastewater effluent (WW effluent).

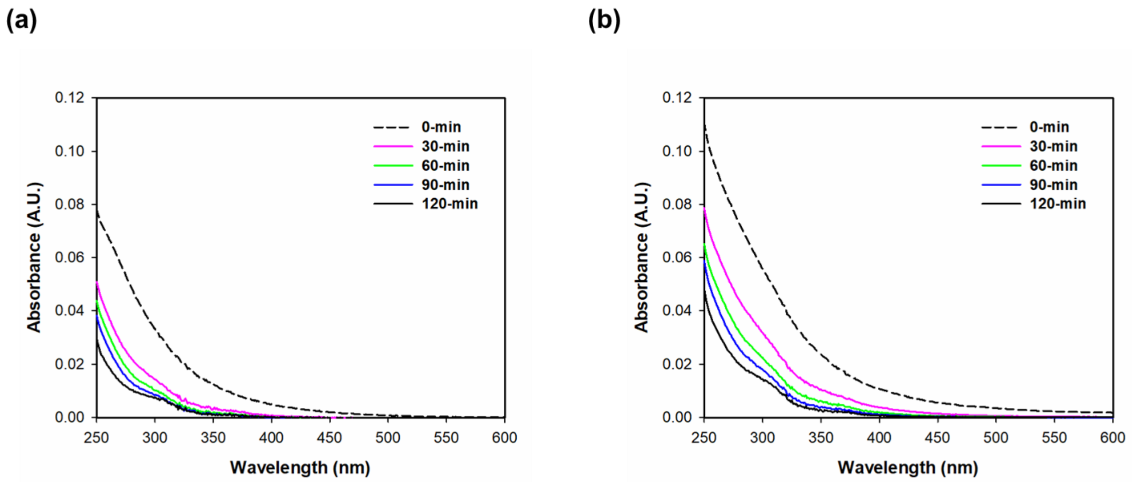

Figure S3. Changes of UV/Vis spectra during the photocatalytic degradation of organic matter with 0.2 g/L of ZnO dosage at pH 7: (a) DOM (upstream sample), and (b) EfOM (wastewater effluent).

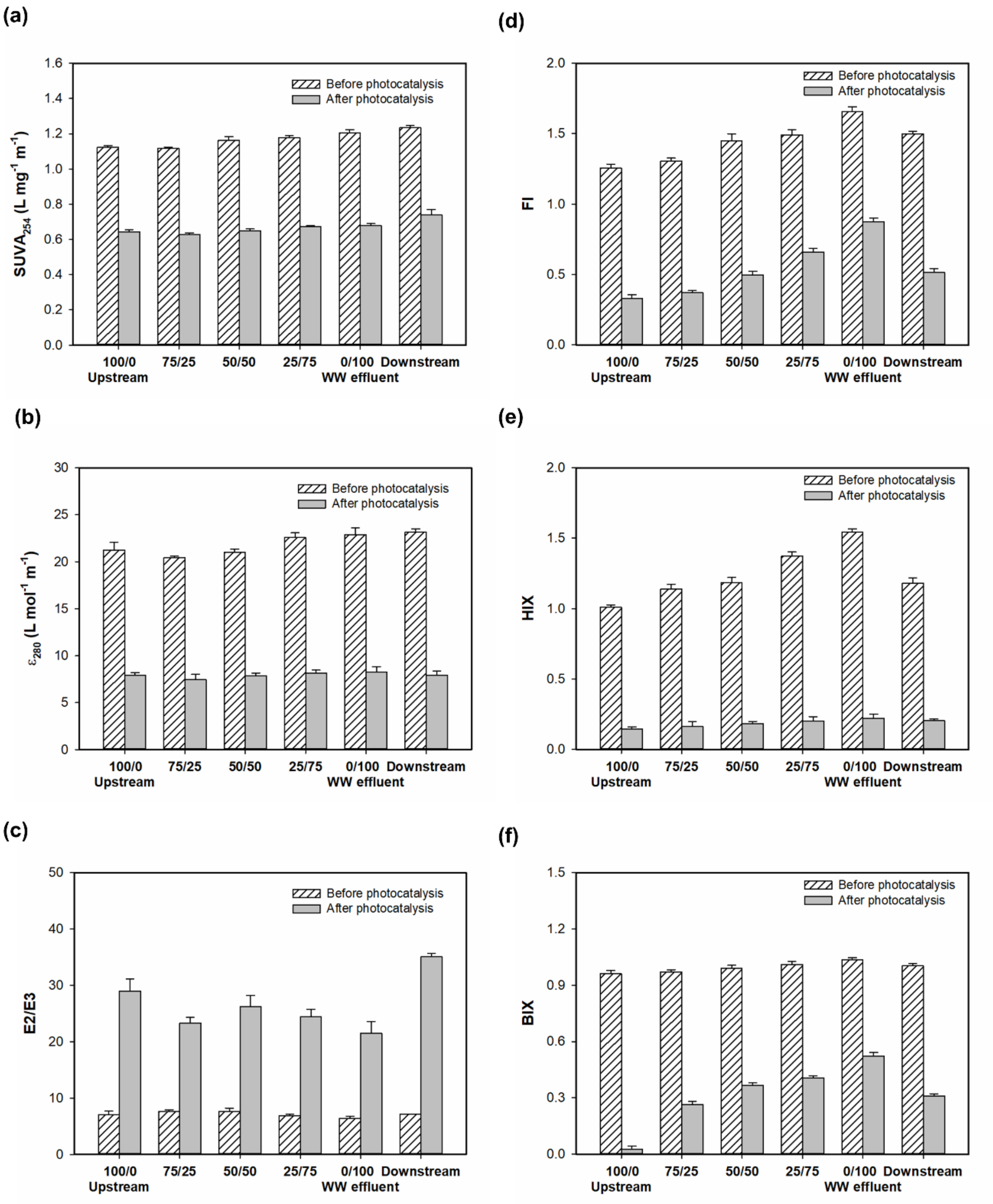

Figure S4. Changes of the optical parameters for upstream, wastewater effluent, and downstream samples by photocatalysis with 0.2 g/L of ZnO at pH 7: (**a**) $SUVA_{254}$, (**b**) $\boldsymbol{\varepsilon_{280}}$, (**c**) E2/E3, (**d**) FI, (**e**) HIX, and (**f**) BIX.

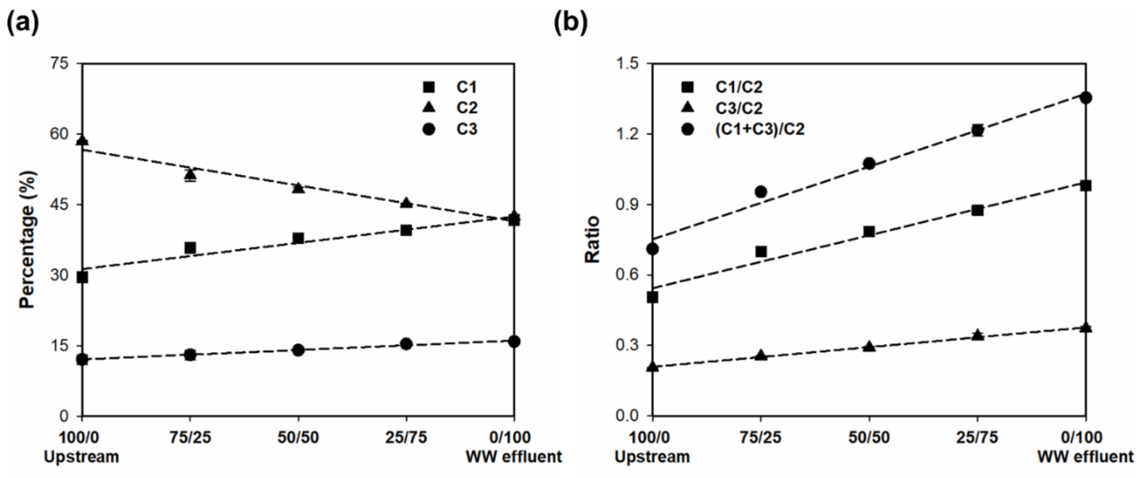

Figure S5. Changes in the relative distribution of PARAFAC components during the mixing between upstream and wastewater effluent: (**a**) Percentage contribution (%) and (**b**) PARAFAC component ratios.

List of Tables

Table S1. Basic water properties of upstream, wastewater effluent, and downstream samples

Sample Type	DOC (mg/L)	UV_{254} (A.U.)	$SUVA_{254}$ (L/mg-m)	FI	HIX	BIX	pH	Conductivity (μS/cm)	TN (mg/L)
Upstream of WWTP (DOM)	6.51	0.0729	1.119	1.28	1.01	0.93	6.83	394	9.85
	6.48	0.0734	1.133	1.24	1.01	1.00	6.80	391	9.94
	6.53	0.0732	1.121	1.25	1.00	0.96	6.89	392	9.94
	6.51	**0.0732**	**1.124**	**1.26**	**1.01**	**0.96**		**392.3**	**9.91**
Wastewater effluent (EfOM)	8.52	0.1022	1.199	1.65	1.55	1.03	6.68	567	14.55
	8.54	0.1019	1.193	1.63	1.42	1.04	6.64	565	14.77
	8.55	0.1045	1.223	1.69	1.38	1.04	6.67	571	14.80
	8.54	**0.1029**	**1.205**	**1.66**	**1.45**	**1.04**		**567.7**	**14.70**
Downstream of WWTP	8.10	0.0990	1.223	1.50	1.18	1.00	6.89	430	9.24
	7.98	0.0994	1.246	1.50	1.19	1.00	6.96	429	9.36
	8.05	0.0992	1.232	1.49	1.17	1.00	6.97	425	9.34
	8.04	**0.0992**	**1.234**	**1.50**	**1.18**	**1.00**		**428.0**	**9.31**

Table S2. Spectral characteristics of the three PARAFAC components identified by PARAFAC in this study and the comparison with those previously identified. The maxima wavelengths are presented in excitation/emission wavelengths.

Components	Ex_{max}/Em_{max}	Traditional peaks [1]	Comparison with other studies using PARAFAC	Description	Reference
C1	≤230(325)nm/406nm	"A" peak: 260/380-460 "M" peak: 312/380-420	C6:<250(300)/406: Marine and terrestrial humic substances	Humic-like component	[2]
			C3: An intermediate that is formed as a result of the photochemical degradation of terrestrial DOM		[3]
			C2: <240(340)/398: Humic-like fluorescence		[4]
			P1: (< 260)310/414: Marine and terrestrial humic materials		[5]
			C1: 240(310)/429.5: Humic-like component (peaks A + M)		[6]
			G2: <250,320/400: Microbial humic-like fluorescence		[7]
			C2: 305(<250)/400: Microbial humic-like		[8]
			C2: 250,310/400: Humic-like component		[9]
			C1: 230,330/420: Terrestrial humic-like		[10]
			C2: ≤240, 300/408 nm: Microbial humic-like substances		[11]
C2	≤230(276)nm/304nm	"B" peak: 275/310	Component 8: 275/304: Tyrosine-like fluorescence	Tyrosine-like component	[12]
			C4: 275/306: Tyrosine-like fluorescence		[13]
			C1/P5: Tyrosine-like fluorescence		[5]
			Tyrosine-like fluorescence		[13]
			C7: Tyrosine-like fluorescence		[14]
			G4: 250/304: Protein - tyrosine-like		[7]
			C2: 275(290)/306: Protein-like (tyrosine-like) components		[15]
C3	261nm/490nm	"A" peak: 260/380-460 "C" peak: 350/420-480	C1:260(360)/480: Terrestrial humic substances	Terrestrial-like humic substances	[2]
			P3:<260(380)/498: Terrestrial humic substances		[5]
			C3:260(370)/490: Terrestrial humic substances		[16]
			C4: 265(370)/490: Terrestrial-like humic substances		[17]
			C4: 270(390)/508: Terrestrial-like humic substances		[18]
			C4: 250(360)/500: Humic-like organic matter		[19]
			C5: 270(400)/490: Microbial humic-like		[20]

Table S3. Pearson's correlation coefficients between selected parameters for upstream, wastewater effluent, and downstream samples

	DOC	UV_{254}	$SUVA_{254}$	ε_{280}	$S_{275-295}$	S_R	E2/E3	FI	HIX	BIX	%C1	%C2	%C3
DOC	1												
UV_{254}	0.984	1											
$SUVA_{254}$	0.826	0.913	1										
ε_{280}	0.651	0.707	0.748	1									
$S_{275-295}$	0.634	0.661	0.626	0.767	1								
S_R	-0.642	-0.650	-0.576	-0.637	-0.903	1							
E2/E3	-0.323	-0.306	-0.222	-0.689	-0.610	0.317	1						
FI	0.963	0.938	0.764	0.604	0.606	-0.603	-0.340	1					
HIX	0.869	0.807	0.566	0.529	0.658	-0.668	-0.375	0.872	1				
BIX	0.861	0.849	0.719	0.659	0.724	-0.621	-0.511	0.833	0.863	1			
%C1	0.801	0.702	0.400	0.320	0.436	-0.504	-0.243	0.789	0.929	0.755	1		
%C2	-0.810	-0.716	-0.425	-0.350	-0.469	0.524	0.269	-0.809	-0.948	-0.781	-0.996	1	
%C3	0.802	0.730	0.480	0.423	0.543	-0.557	-0.335	0.831	0.964	0.822	0.944	-0.969	1

Table S4. Flow data at the points where we collected the upstream and downstream samples for three months in 2019. Unit: m^3/s (*Source: Han River Flood Control Office*).

Date	Upstream	Downstream	Date	Upstream	Downstream	Date	Upstream	Downstream	Date	Upstream	Downstream
2019/05/01	265.44	400	2019/06/01	189.92	376.37	2019/07/01	153.95	409.17	2019/08/01	1600.38	2458.55
2019/05/02	239.42	437.73	2019/06/02	164.74	454.86	2019/07/02	158.28	570.49	2019/08/02	1045.48	2009.47
2019/05/03	269.58	547.2	2019/06/03	197.58	580.31	2019/07/03	171.46	743.95	2019/08/03	498.08	1557.76
2019/05/04	220.05	560.41	2019/06/04	252.77	679.79	2019/07/04	152.01	811.23	2019/08/04	564.1	1535.39
2019/05/05	181.11	661.72	2019/06/05	311.14	874.3	2019/07/05	147.93	871.3	2019/08/05	452.74	1317.23
2019/05/06	191.78	652.88	2019/06/06	235.87	786.99	2019/07/06	166.35	875.23	2019/08/06	205.36	918.48
2019/05/07	148.72	787.83	2019/06/07	463.09	934.88	2019/07/07	246.22	792.14	2019/08/07	508.21	1026.13
2019/05/08	259.6	777.32	2019/06/08	703.59	865.53	2019/07/08	182.86	623.9	2019/08/08	722.98	949.09
2019/05/09	278.05	551.87	2019/06/09	442.29	801.05	2019/07/09	166.77	471.63	2019/08/09	397.09	472.93
2019/05/10	259.76	536.71	2019/06/10	253.63	504.87	2019/07/10	157.91	383.96	2019/08/10	529.53	510.23
2019/05/11	170.51	436.2	2019/06/11	211.14	338.86	2019/07/11	204.04	346.48	2019/08/11	322.65	425.28
2019/05/12	211.18	332.66	2019/06/12	265.01	333.85	2019/07/12	204.17	290.87	2019/08/12	646.36	743.71
2019/05/13	212.7	298.34	2019/06/13	212.7	355.53	2019/07/13	183.16	305.65	2019/08/13	974.74	1119.03
2019/05/14	258.04	360.29	2019/06/14	215.85	391.86	2019/07/14	160.85	368.44	2019/08/14	631.13	1012.48
2019/05/15	185.41	344.94	2019/06/15	258.74	506.62	2019/07/15	256.4	438.3	2019/08/15	560.83	992.97
2019/05/16	166.81	421.57	2019/06/16	161.97	566.92	2019/07/16	246.59	540.98	2019/08/16	478.73	1133.8
2019/05/17	82.42	557.98	2019/06/17	224.98	649.74	2019/07/17	171.16	520.73	2019/08/17	419.26	1136.73
2019/05/18	184.71	715.05	2019/06/18	196.92	742.39	2019/07/18	156.67	558.94	2019/08/18	460.69	1081.74
2019/05/19	273.33	808.45	2019/06/19	184.62	763.94	2019/07/19	161.06	574.24	2019/08/19	378.66	941.05
2019/05/20	208.53	987.64	2019/06/20	281.53	694.42	2019/07/20	204.12	562.22	2019/08/20	320.47	776.26
2019/05/21	208.54	733.82	2019/06/21	305.29	638.9	2019/07/21	202.56	542.97	2019/08/21	295.51	601.85
2019/05/22	200.71	710.95	2019/06/22	227.96	510.89	2019/07/22	183.93	498.46	2019/08/22	260.11	553.49
2019/05/23	250.23	547.91	2019/06/23	200.76	404.53	2019/07/23	169.84	409.53	2019/08/23	246.91	432.98
2019/05/24	192.88	399.34	2019/06/24	198.27	332.04	2019/07/24	265.15	453.88	2019/08/24	231.91	378.99
2019/05/25	199.38	314.98	2019/06/25	209.71	276.17	2019/07/25	321.71	455.49	2019/08/25	190.07	285.22
2019/05/26	225.99	268.5	2019/06/26	289.67	252.47	2019/07/26	1144.39	962.29	2019/08/26	217.52	294.63
2019/05/27	308.7	315.73	2019/06/28	211.08	233.82	2019/07/27	1647.11	1314.61	2019/08/27	285.41	308.73
2019/05/28	279.54	284.44	2019/06/29	222.69	292.44	2019/07/28	1224.64	1065.41	2019/08/28	267.7	412.91
2019/05/29	215.83	246.48	2019/06/30	189.83	337.85	2019/07/29	577.13	690.3	2019/08/29	458.77	859.4
2019/05/30	215.91	252.47				2019/07/30			2019/08/30		
2019/05/31	211.64	280.11				2019/07/31					

Table S5. Discharge volume from the wastewater treatment plant into the Han river in 2019 (*Source: Seoul Metropolitan Government*).

Months	Municipal wastewater treatment plant flowrate (ton/day)		
	Process 1	Process 2	Summary
January	506,521	939,791	1,446,312
February	510,419	952,395	1,462,814
March	503,810	970,002	1,473,812
April	530,063	966,352	1,496,415
May	532,940	967,388	1,500,328
June	547,116	1,018,408	1,565,524
July	620,429	1,066,965	1,687,394
August	668,688	1,095,540	1,764,228
September	633,813	1,076,323	1,710,136
October	591,380	952,115	1,543,495
November	671,718	920,887	1,592,605
December	726,420	749,171	1,475,591

References

1. Coble, P.G. Characterization of marine and terrestrial DOM in seawater using excitation-emission matrix spectroscopy. *Mar. Chem.* **1996**, *51*, 325–346.
2. Baghoth, S.A.; Sharma, S.K.; Amy, G.L. Tracking natural organic matter (NOM) in a drinking water treatment plant using fluorescence excitation-emission matrices and PARAFAC. *Water Res.* **2011**, *45*, 797–809; DOI: 10.1016/j.watres.2010.09.005.
3. Stedmon, C.A; Markager, S.; Tranvik, L.; Kronberg, L.; Slätis, T.; Martinsen, W. Photochemical production of ammonium and transformation of dissolved organic matter in the Baltic Sea. *Mar. Chem.* **2007**, *104*, 227–240; DOI: 10.1016/j.marchem.2006.11.005.
4. Stedmon, C.A.; Markager, S. Tracing the production and degradation of autochthonous fractions of dissolved organic matter by fluorescence analysis. *Limnol. Oceanogr.* **2005**, *50*, 1415–1426; DOI: 10.4319/lo.2005.50.5.1415.
5. Murphy, K.R.; Stedmon, C.A.; Waite, T.D.; Ruiz, G.M. Distinguishing between terrestrial and autochthonous organic matter sources in marine environments using fluorescence spectroscopy. *Mar. Chem.* **2008**, *108*, 40–58; DOI: 10.1016/j.marchem.2007.10.003.
6. García, P.E.; García, R.D.; Cárdenas, C.S.; Gerea, M.; Reissig, M.; Pérez G.L.; Stefano, L.G.D.; Gianello, D.; Queimaliños, C.; Diéguez, M.C. Fluorescence components of natural dissolved organic matter (DOM) from aquatic systems of an Andean Patagonian catchment: Applying different data restriction criteria for PARAFAC modelling. *Spectrochim. Acta - Part A Mol. Biomol. Spectrosc.* **2020**, *229*, 117957; DOI: 10.1016/j.saa.2019.117957.
7. Murphy, K.R.; Hambly, A.; Singh, S.; Henderson, R.K.; Baker, A.; Stuetz, R.; Khan, S.J. Organic Matter Fluorescence in Municipal Water Recycling Schemes: Toward a Unified PARAFAC Model. *Environ. Sci. Technol.* **2011**, *45*, 2909–2916; DOI: 10.1021/es103015e.
8. Osburn, C.L.; Wigdahl, C.R.; Fritz, S.C.; Saros, J.E. Dissolved organic matter composition and photoreactivity in prairie lakes of the U.S. Great Plains. *Limnol. Oceanogr.* **2011**, *56*, 2371–2390; DOI: 10.4319/lo.2011.56.6.2371.
9. Watson, K.; Farré, M.J.; Leusch, F.D.L.; Knight, N. Using fluorescence-parallel factor analysis for assessing disinfection by-product formation and natural organic matter removal efficiency in secondary treated synthetic drinking waters. *Sci. Total Environ.* **2018**, *640-641*, 31–40; DOI: 10.1016/j.scitotenv.2018.05.280.
10. Kothawala, D.N.; Stedmon, C.A.; Müller, R.A.; Weyhenmeyer, G.A.; Köhler, S.J.; Tranvik, L.J. Controls of dissolved organic matter quality: evidence from a large-scale boreal lake survey. *Glob. Chang. Biol.* **2014**, *20*, 1101–1114; DOI: 10.1111/gcb.12488.
11. Yang, L.; Chen, W.; Zhuang, W.-E.; Cheng, Q.; Li, W.; Wang, H.; Guo, W.; Chen, C.A.; Liu, M. Characterization and bioavailability of rainwater dissolved organic matter at the southeast coast of China using absorption spectroscopy and fluorescence EEM-PARAFAC. *Estuar. Coast. Shelf Sci.* **2019**, *217*, 45–55; DOI: 10.1016/j.ecss.2018.11.002.
12. Stedmon, C.A.; Markager, S. Resolving the variability in dissolved organic matter fluorescence in a temperate estuary and its catchment using PARAFAC analysis. *Limnol. Oceanogr.* **2005**, *50*, 686–697; DOI: 10.4319/lo.2005.50.2.0686
13. Yamashita, Y.; Cory, R.M.; Nishioka, J.; Kuma, K.; Tanoue, E.; Jaffé, R. Fluorescence characteristics of dissolved organic matter in the deep waters of the Okhotsk Sea and the northwestern North Pacific Ocean. *Deep. Res. Part II Top. Stud. Oceanogr.* **2010**, *57*, 1478–1485; DOI: 10.1016/j.dsr2.2010.02.016.
14. Yamashita, Y.; Jaffé, R.; Maie, N.; Tanoue, E. Assessing the dynamics of dissolved organic matter (DOM) in coastal environments by excitation emission matrix fluorescence and parallel factor analysis (EEM-PARAFAC). *Limnol. Oceanogr.* **2008**, *53*, 1900–1908; DOI: 10.4319/lo.2008.53.5.1900
15. Hu, H.; Ren, H. Can fluorescence spectrometry be used as a surrogate for predicting the dissolved organic nitrogen and its bioavailable portion in wastewater effluents? *Chemosphere* **2016**, *164*, 299–303; DOI: 10.1016/j.chemosphere.2016.08.080
16. Murphy, K.R.; Ruiz, G.M.; Dunsmuir, W.T.M.; Waite, T.D. Optimized Parameters for Fluorescence-Based Verification of Ballast Water Exchange by Ships. *Environ. Sci. Technol.* **2006**, *40*, 2357–2362; DOI: 10.1021/es0519381.

17. Phong, D.D.; Hur, J. Insight into photocatalytic degradation of dissolved organic matter in UVA/TiO_2 systems revealed by fluorescence EEM-PARAFAC. *Water Res.* **2015**, *87*, 119–126; DOI: 0.1016/j.watres.2015.09.019.
18. Kowalczuk, P.; Durako, M.J.; Young, H.; Kahn, A.E.; Cooper, W.J.; Gonsior, M. Characterization of dissolved organic matter fluorescence in the South Atlantic Bight with use of PARAFAC model: Interannual variability. *Mar. Chem.* **2009**, *113*, 182–196; DOI: 10.1016/j.marchem.2009.01.015.
19. Ahn, Y.; Lee, D.; Kwon, M.; Choi, I.-H.; Nam, S.-N.; Kang, J. W. Characteristics and fate of natural organic matter during UV oxidation processes. Chemosphere **2017**, *184*, 960–968; DOI: 10.1016/j.chemosphere.2017.06.079.
20. Yan, M.; Fu, Q.; Li, D.; Gao, G.; Wang, D. Study of the pH influence on the optical properties of dissolved organic matter using fluorescence excitation-emission matrix and parallel factor analysis. *J. Lumin.* **2013**, *142*, 103–109; DOI: 10.1016/j.jlumin.2013.02.052.